Production of the doubly heavy baryons at the hadronic colliders

Xing-Gang Wu
Department of Physics, Chongqing University
Chao-Hsi Chang
Institute of Theoretical Physics, Chinese Academy of Science

In collaboration with *Cong-Feng Qiao*, *Jian-Ping Ma*, *Jian-Xiong Wang*, *Xian-You Wang*, *Jun Jiang*, *Jia-Wei Zhang*, *Gu Chen*, and etal.

CERN, 8-10, Nov., Implications of LHCb measurements and future prospects

Outlines

1. Background
2. Generator GENXICC
3. Properties of hadroproduction of Xicc/Xibc
   - Results for Xicc/Xibc at the LHC
   - Results for Xicc at the After@LHC

   Different measurements
4. Summary

1. Background

theoretical predictions. The theoretical estimates predicted that, of the total sample at the fixed target experiment SELEX, about 10^{-5} of Λ_c^+ events would be produced via Ξ_{cc}^+ decay accordingly [4–8], whereas, the SELEX collaboration found that almost 20% of Λ_c^+ events in their sample were produced via Ξ_{cc}^+ decay.

Phys. Rev. Lett. 89, 112001 (2002)

$\Xi_{cc}^+ \to \Lambda_c^+ K^- \pi^+$

Roughly 10^4 larger than expected

We observe a signal for the doubly charmed baryon Ξ_{cc}^+ in the decay mode $\Xi_{cc}^+ \to pD^+K^-$ to complement the previous reported decay $\Xi_{cc}^+ \to \Lambda_c^+ K^- \pi^+$ in data from SELEX, the charm hadro-production experiment at Fermilab. In this new decay mode we

In Ref. [1] we noted that the $\Xi_{cc}^+ \to \Lambda_c^+ K^- \pi^+$ yield and acceptance implied that a large fraction of the Λ_c^+ decays seen in SELEX came from double charm decays. That was a surprise. For the $\Xi_{cc}^+ \to pD^+K^-$ case that is not true. Only a few percent of the SELEX D^+ events are associated with double charm.

Phys.Lett.B628, 18 (2005)

SELEX is still the only experiment observing double charm baryons. We published observations on two different decays modes, $\Xi_{cc}^+ \to \Lambda_c^+ K^- \pi^+$ [5] and $\Xi_{cc}^+ \to p D^+ K^-$ [12]. After a re-analysis of our full data set, with improved efficiency and resolution, we presented here a higher-statistics observation of $\Xi_{cc}^+ \to \Lambda_c^+ K^- \pi^+$, and a re-analysis of the $\Xi_{cc}(3780)^{++}$. The new analysis also allows access to additional decay modes, and we presented here the first observation of $\Xi_{cc}^+ \to \Xi_c^+ \pi^- \pi^+$.

SELEX, arXiv:0702001

other experiments

essential to observe the same state in some other way. Other experiments with large charm baryon samples, e.g., the FOCUS [7] and E791 fixed target charm experiments at Fermilab or the B-factories, have not confirmed the double charm signal. This is

A search for the doubly charmed baryon Ξ_{cc}^+ in the decay mode $\Xi_{cc}^+ \to \Lambda_c^+ K^- \pi^+$ is performed with a data sample, corresponding to an integrated luminosity of 0.65 fb^{-1}, of pp collisions recorded at a centre-of-mass energy of 7 TeV. No significant signal is found in the mass range 3300–3800 MeV/c^2. Upper limits at the 95% confidence level on the ratio of the Ξ_{cc}^+ production cross-section times branching fraction to that of the Λ_c^+, R, are given as a function of the Ξ_{cc}^+ mass and lifetime. The largest upper limits range from $R < 1.5 \times 10^{-2}$ for a lifetime of 100 fs to $R < 3.9 \times 10^{-4}$ for a lifetime of 400 fs.

LHCb,JHEP12,090(2013)

There is still no definite conclusions on SELEX 02 results

What's the argument for the conclusion of

about 10^{-5} of Λ_c^+ events would be produced via Ξ_{cc}^+ decay

At high energies of parton subprocesses as the gluon fusion $gg \to cc\bar{c}\bar{c}$, the hard production of heavy quarks is suppressed in comparison with the production of single pair $c\bar{c}$ by the factor of 10^{-2}

The gluon fusion dominant at the SELEX energies, the hard production supposes a strong threshold effect for four heavy quarks. This threshold suppression is significant and results in the additional factor of 10^{-2}

The hadronization of four heavy quarks results in a fraction of doubly heavy baryons about 10^{-1}

Such naive order estimation is correct or not ?

The production cross-section could be small, but cannot be too small

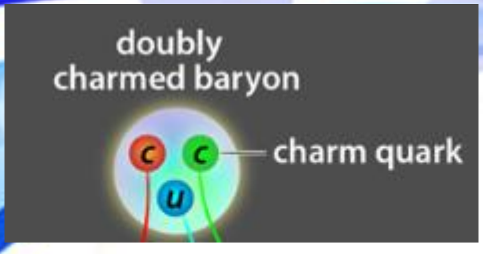

LHCb new measurements

A highly significant structure is observed in the $\Lambda_c^+ K^- \pi^+ \pi^+$ mass spectrum, where the Λ_c^+ baryon is reconstructed in the decay mode $pK^-\pi^+$. The structure is consistent with originating from a weakly decaying particle, identified as the doubly charmed baryon Ξ_{cc}^{++}. The difference between the masses of the Ξ_{cc}^{++} and Λ_c^+ states is measured to be $1334.94 \pm 0.72(\text{stat.}) \pm 0.27(\text{syst.})\ \text{MeV}/c^2$, and the Ξ_{cc}^{++} mass is then determined to be $3621.40 \pm 0.72(\text{stat.}) \pm 0.27(\text{syst.}) \pm 0.14(\Lambda_c^+)\ \text{MeV}/c^2$, where the last uncertainty is due to the limited knowledge of the Λ_c^+ mass. The state is observed in a sample of proton-proton collision data collected by the LHCb experiment at a center-of-mass energy of 13 TeV, corresponding to an integrated luminosity of $1.7\ \text{fb}^{-1}$, and confirmed in an additional sample of data collected at 8 TeV.

A longer lifetime

A large branching fraction - See Wei Wang's talk

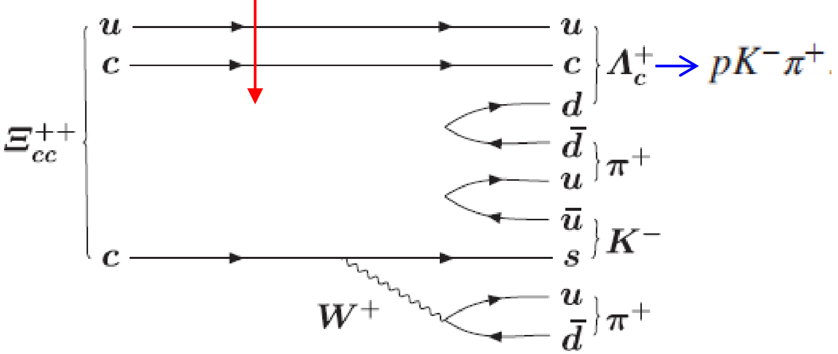

Maybe 5fb^{-1}

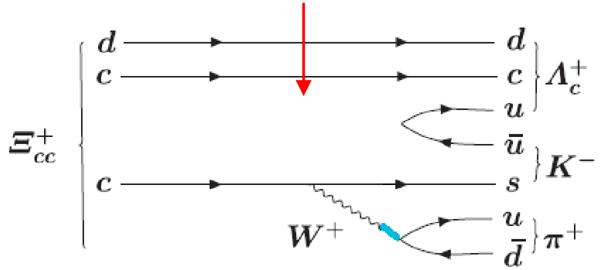

What's the more accurate production mechanism (our main concern)

I) Production mechanisms、
II) More intermediate baryon states/combinations、
III) Treatment in specific kinematic regions、

pQCD calculable

Hard quark pair

We show that from the production side alone, the "seemingly" gap could be changed from 2×10^4 down to 10^2; Maybe carefully studies on the decay part (mostly non-perturbative, still with large uncertainty) may finally solve the puzzle.

The use of typical fragmentation function gives negligible differences.

$$D^H_{QQ'}(z) = \frac{N_{QQ'}}{z[1-(1/z)-\epsilon_{QQ'}/(1-z)]^2},$$

The hadronic production mechanisms for Xicc

(General picture: Production of a charm diquark pair first, and the diquark fragment into baryon with 100% efficiency)

gg-channel

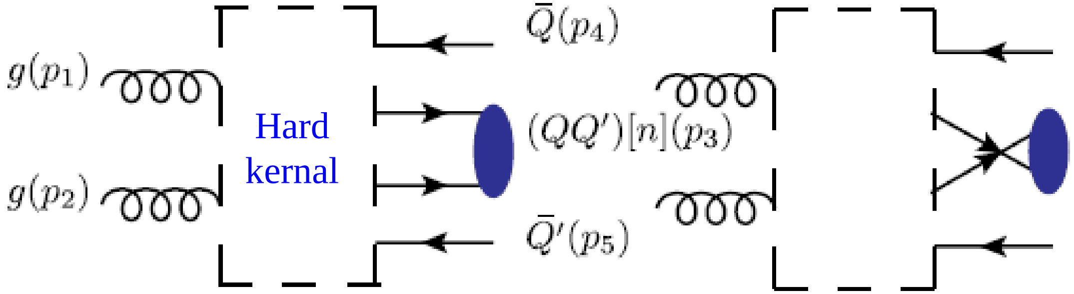

gc-channel

cc-channel

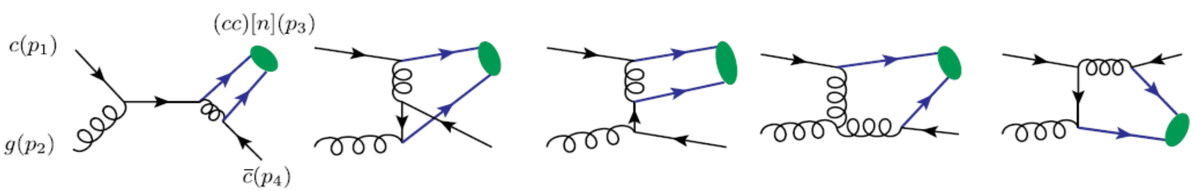

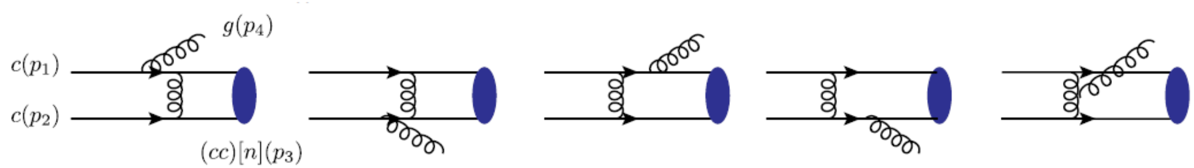

1) gluon-gluon fusion mechanism (dominant; main concern)

$g+g\to(cc)[^3S_1]_{\bar{3}}+\bar{c}+\bar{c}$, $g+g\to(cc)[^1S_0]_6+\bar{c}+\bar{c}$

2) gluon-charm collision mechanism

$g+c\to(cc)[^3S_1]_{\bar{3}}+\bar{c}$, $g+c\to(cc)[^1S_0]_6+\bar{c}$

3) charm-charm collision mechanism

$c+c\to(cc)[^3S_1]_{\bar{3}}+g$, $c+c\to(cc)[^1S_0]_6+g$

Here, charm is either extrinsic or intrinsic

Lund model: u:d:s=1:1:0.3

$\Xi_{cc}^{++}:\Xi_{cc}^{+}:\Omega_{cc}^{+}=43\%:43\%:16\%$

Two-body phase-space, significant in lower-p_t region

Table 1
All the considered channels for the hadronic production of the double-heavy baryon, which are defined by the two parameters **mgenxi** and **ixiccstate**. Here the symbol gg-channel stands for the gluon–gluon fusion channel, etc.

	mgenxi=1 (for Ξ_{cc})	mgenxi=2 (for Ξ_{bc})	mgenxi=3 (for Ξ_{bb})
ixiccstate=1	gg-channel, $(cc)_{\bar{3}}(^3S_1)$	gg-channel, $(bc)_{\bar{3}}(^3S_1)$	gg-channel, $(bb)_{\bar{3}}(^3S_1)$
ixiccstate=2	gg-channel, $(cc)_6(^1S_0)$	gg-channel, $(bc)_6(^1S_0)$	gg-channel, $(bb)_6(^1S_0)$
ixiccstate=3	gc-channel, $(cc)_{\bar{3}}(^3S_1)$	gg-channel, $(bc)_6(^3S_1)$	–
ixiccstate=4	gc-channel, $(cc)_6(^1S_0)$	gg-channel, $(bc)_{\bar{3}}(^1S_0)$	–
ixiccstate=5	cc-channel, $(cc)_{\bar{3}}(^3S_1)$	–	–
ixiccstate=6	cc-channel, $(cc)_6(^1S_0)$	–	–

2. Xicc Generator GENXICC

Analog

$$gg \rightarrow (c+c)\Xi_{cc} + \bar{c} + \bar{c}$$

$$gg \rightarrow (c+\bar{b})B_c^+ + \bar{c} + b$$

BCVEGPY

Key transformation: $\bar{b}$-quark line to c-quark line

Main Differences for Xicc and Bc productions

$$u_s(r) = \frac{1}{\sqrt{2r\cdot q}}(\not{q}+m)|q_h\rangle$$

$$v_s(r) = \frac{1}{\sqrt{2r\cdot q}}(\not{q}-m)|q_{-h}\rangle$$

The spin of massive spinor corresponds to helicity of an arbitrary massless spinor

The arbitrary massless spinor could be a test of the correctness of program

Transforming quark-line to anti-quark line

$$\mathrm{HME}_i = \langle q_{0\lambda_2}|(\not{p}_{c4}+m_c)\hat{\Gamma}_i(\not{p}_{c3}-m_c)|q_{0\lambda_1}\rangle,$$

$$\mathrm{HME}_i = -\langle q_{0(-\lambda_1)}|(\not{p}_{c3}+m_c)\Gamma_i(\not{p}_{c4}-m_c)|q_{0(-\lambda_2)}\rangle.$$

$$\langle p_{(\lambda_1)}|\not{k}_1\ldots\not{k}_n|q_{(\lambda_2)}\rangle = (-1)^{n+1}\langle q_{(-\lambda_2)}|\not{k}_n\ldots\not{k}_1|p_{(-\lambda_1)}\rangle,$$

Color factor

TABLE V. The square of the six independent color factors (including the cross terms) for $gg \to (cc)_{\bar{3}}[^3S_1] + \bar{c} + \bar{c}$, $(C_{mij} \times C^*_{nij})$ with $m, n = (1, 2, \cdots, 6)$, respectively.

	C^*_{1ij}	C^*_{2ij}	C^*_{3ij}	C^*_{4ij}	C^*_{5ij}	C^*_{6ij}
C_{1ij}	$\frac{4}{3}$	$-\frac{1}{6}$	$\frac{2}{3}$	$-\frac{1}{12}$	$\frac{5}{12}$	$-\frac{1}{3}$
C_{2ij}	$-\frac{1}{6}$	$\frac{4}{3}$	$-\frac{1}{12}$	$\frac{2}{3}$	$-\frac{1}{3}$	$\frac{5}{12}$
C_{3ij}	$\frac{2}{3}$	$-\frac{1}{12}$	$\frac{4}{3}$	$-\frac{5}{12}$	$\frac{1}{12}$	$-\frac{2}{3}$
C_{4ij}	$-\frac{1}{12}$	$\frac{2}{3}$	$-\frac{5}{12}$	$\frac{4}{3}$	$-\frac{2}{3}$	$\frac{1}{12}$
C_{5ij}	$\frac{5}{12}$	$-\frac{1}{3}$	$\frac{1}{12}$	$-\frac{2}{3}$	$\frac{4}{3}$	$-\frac{1}{6}$
C_{6ij}	$-\frac{1}{3}$	$\frac{5}{12}$	$-\frac{2}{3}$	$\frac{1}{12}$	$-\frac{1}{6}$	$\frac{4}{3}$

TABLE VI. The square of the six independent color factors (including the cross terms) for $gg \to (cc)_6[^1S_0] + \bar{c} + \bar{c}$, $(C_{mij} \times C^*_{nij})$ with $m, n = (1, 2, \cdots, 6)$, respectively.

	C^*_{1ij}	C^*_{2ij}	C^*_{3ij}	C^*_{4ij}	C^*_{5ij}	C^*_{6ij}
C_{1ij}	$\frac{8}{3}$	$-\frac{1}{3}$	$\frac{2}{3}$	$-\frac{1}{12}$	$\frac{11}{12}$	$\frac{1}{6}$
C_{2ij}	$-\frac{1}{3}$	$\frac{8}{3}$	$-\frac{1}{12}$	$\frac{2}{3}$	$\frac{1}{6}$	$\frac{11}{12}$
C_{3ij}	$\frac{2}{3}$	$-\frac{1}{12}$	$\frac{8}{3}$	$\frac{11}{12}$	$-\frac{1}{12}$	$\frac{2}{3}$
C_{4ij}	$-\frac{1}{12}$	$\frac{2}{3}$	$\frac{11}{12}$	$\frac{8}{3}$	$\frac{2}{3}$	$-\frac{1}{12}$
C_{5ij}	$\frac{11}{12}$	$\frac{1}{6}$	$-\frac{1}{12}$	$\frac{2}{3}$	$\frac{8}{3}$	$-\frac{1}{3}$
C_{6ij}	$\frac{1}{6}$	$\frac{11}{12}$	$\frac{2}{3}$	$-\frac{1}{12}$	$-\frac{1}{3}$	$\frac{8}{3}$

As a dedicate generator, the key purpose of GENXICC is to achieve high efficiency

“Helicity Amplitude Approach”

List all possibility of the helicity amplitude and get their numerical values before squared

==> Finding out basic diagrams ← using basic quark lines
==> Using those basic units to form basic QED-like diagrams
using gluon-gluon exchange symmetry;
using quark-line exchange symmetry;
==> Transforming all QCD-like diagrams to QED-like ones
via decomposition

Helicity amplitude for the hard scattering process

$E_{m,1,k}$ (m=1-9)

symmetry

$E_{m,j,k}$ (j=1,2,3,4)

combination

B_{Fi}

$$B_{Fi}^{(\lambda_1\lambda_2\lambda_3\lambda_4\lambda_5\lambda_6)}(q_{b1},q_{b2},q_{c1},q_{c2},k_1,k_2) \equiv B_{Fi}^{(k)}(q_{b1},q_{b2},q_{c1},q_{c2},k_1,k_2) = \sum_{m=1}^{9}\sum_{j=1}^{4} f_{i,m,j}E_{m,j,k}$$

m-- 9 function

j --4 type of symmetry

k --64 helicity combination

$$E_{m,j,k+16} = +E^{*}_{m,j,k} \quad (k=(1,\cdots,4),(9,\cdots,12),(37,\cdots,40),(45,\cdots,48))$$
$$= -E^{*}_{m,j,k} \quad (k=(5,\cdots,8),(13,\cdots,16),(33,\cdots,36),(41,\cdots,44))$$

Independent helicity amplitudes

$^1S_0$-8-independent
$^3S_1$-16-independent

TABLE I: The correspondence between $k=1,\cdots,64$ and $\lambda_1=\pm,\lambda_2=\pm,\lambda_3=\pm,\lambda_4=\pm,\lambda_5=\pm,\lambda_6=\pm$, which stand for the helicities of the particles in the process.

k	λ_1	λ_2	λ_3	λ_4	λ_5	λ_6	k	λ_1	λ_2	λ_3	λ_4	λ_5	λ_6	k	λ_1	λ_2	λ_3	λ_4	λ_5	λ_6	k	λ_1	λ_2	λ_3	λ_4	λ_5	λ_6
1	+	+	+	+	+	+	17	−	−	−	−	−	−	33	+	+	−	+	+	+	49	−	−	+	−	−	−
2	+	+	+	+	+	−	18	−	−	−	−	−	+	34	+	+	−	+	+	−	50	−	−	+	−	−	+
3	+	+	+	+	−	+	19	−	−	−	−	+	−	35	+	+	−	+	−	+	51	−	−	+	−	+	−
4	+	+	+	+	−	−	20	−	−	−	−	+	+	36	+	+	−	+	−	−	52	−	−	+	−	+	+
5	+	+	+	−	+	+	21	−	−	−	+	−	−	37	+	+	−	−	+	+	53	−	−	+	+	−	−
6	+	+	+	−	+	−	22	−	−	−	+	−	+	38	+	+	−	−	+	−	54	−	−	+	+	−	+
7	+	+	+	−	−	+	23	−	−	−	+	+	−	39	+	+	−	−	−	+	55	−	−	+	+	+	−
8	+	+	+	−	−	−	24	−	−	−	+	+	+	40	+	+	−	−	−	−	56	−	−	+	+	+	+
9	+	−	−	+	+	+	25	−	+	+	−	−	−	41	+	−	+	+	+	+	57	−	+	−	−	−	−
10	+	−	−	+	+	−	26	−	+	+	−	−	+	42	+	−	+	+	+	−	58	−	+	−	−	−	+
11	+	−	−	+	−	+	27	−	+	+	−	+	−	43	+	−	+	+	−	+	59	−	+	−	−	+	−
12	+	−	−	+	−	−	28	−	+	+	−	+	+	44	+	−	+	+	−	−	60	−	+	−	−	+	+
13	+	−	−	−	+	+	29	−	+	+	+	−	−	45	+	−	+	−	+	+	61	−	+	−	+	−	−
14	+	−	−	−	+	−	30	−	+	+	+	−	+	46	+	−	+	−	+	−	62	−	+	−	+	−	+
15	+	−	−	−	−	+	31	−	+	+	+	+	−	47	+	−	+	−	−	+	63	−	+	−	+	+	−
16	+	−	−	−	−	−	32	−	+	+	+	+	+	48	+	−	+	−	−	−	64	−	+	−	+	+	+

How to get the value for each non-zero helicity amplitude

Nine basic QED-like diagrams

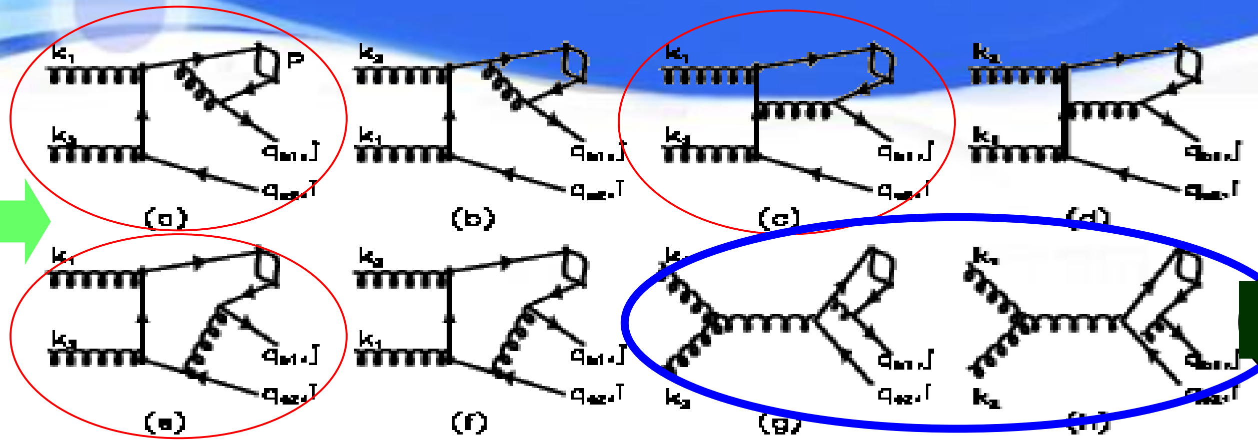

Decompose

Gluon-gluon fusion

…iagrams that can be directly grouped into the cc subset. Here i and j

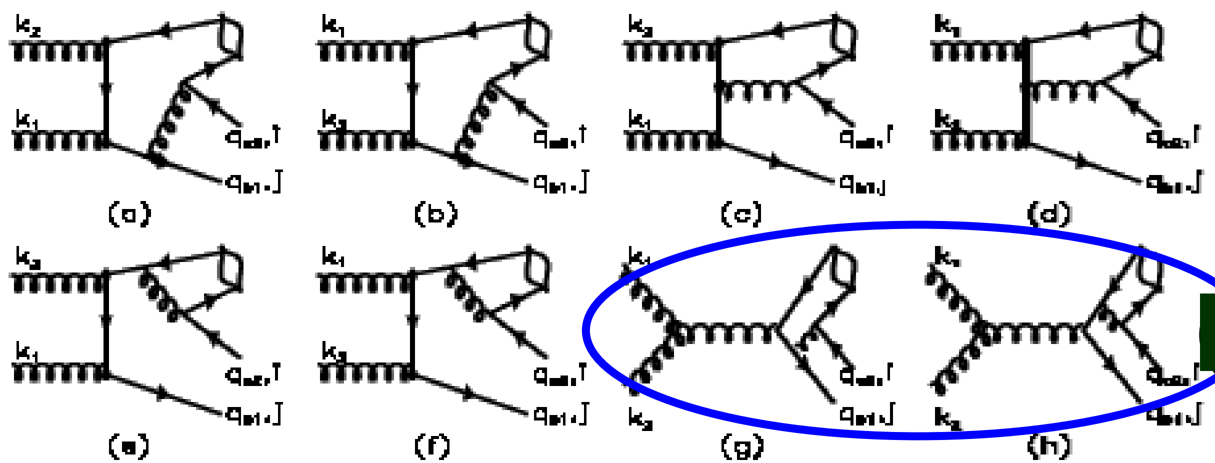

Decompose

Feynman diagrams that can be directly grouped into the bb subset. Here i and j

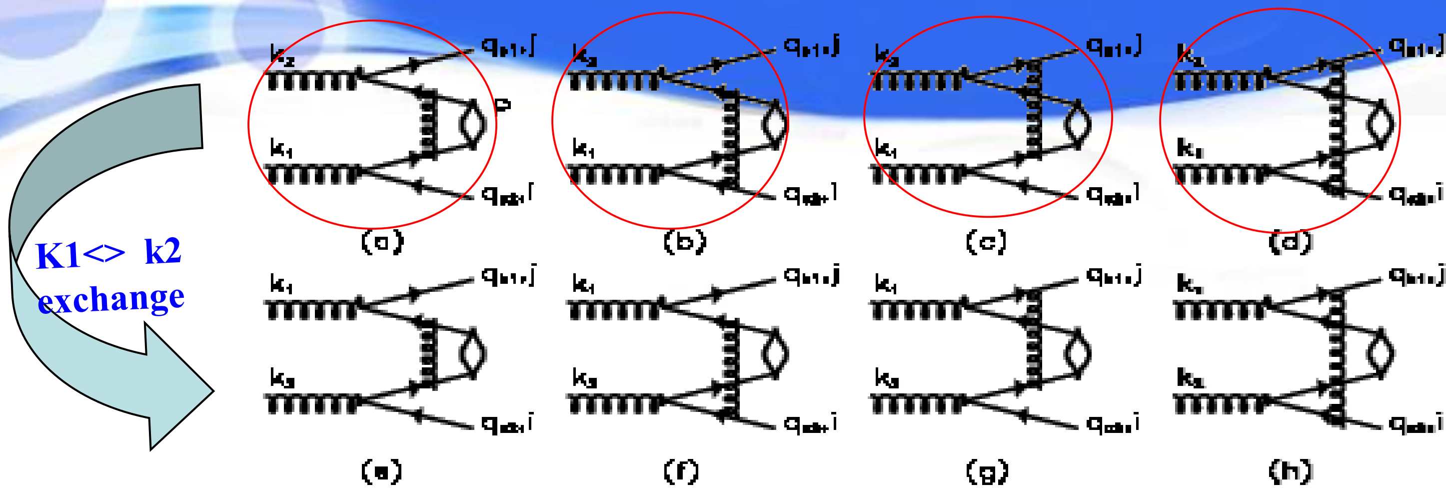

Feynman diagrams that can be directly grouped into the *cb* or *bc* subsets, where

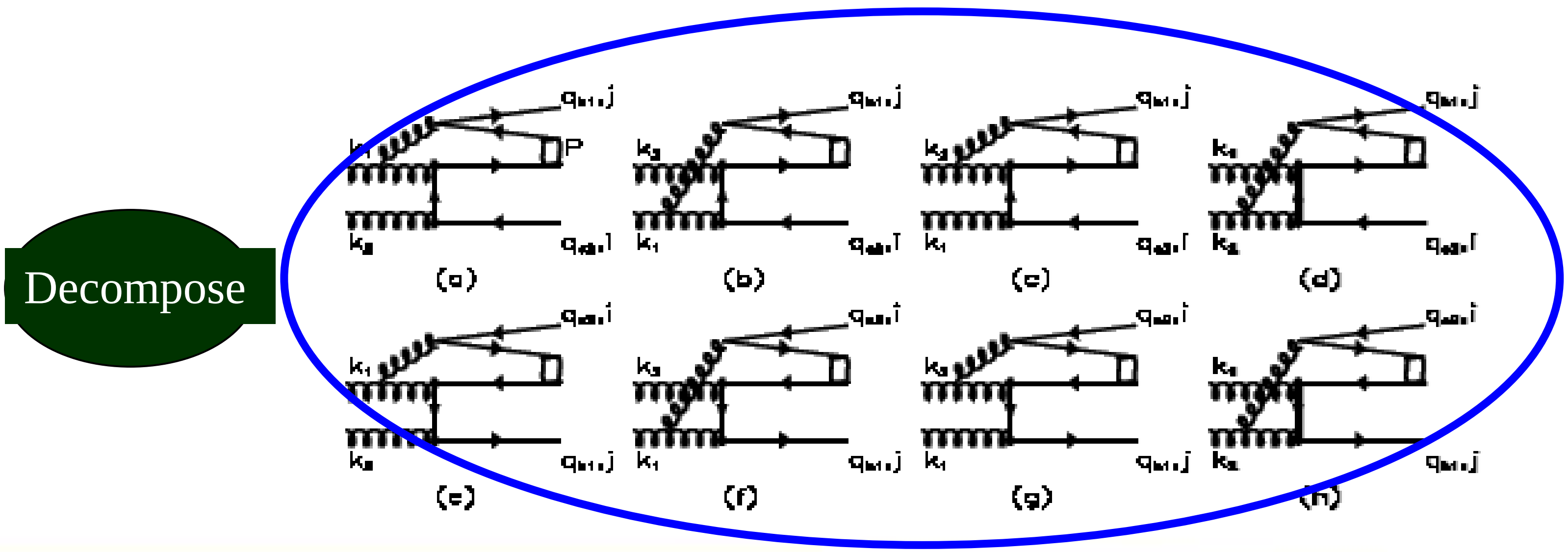

Decompose

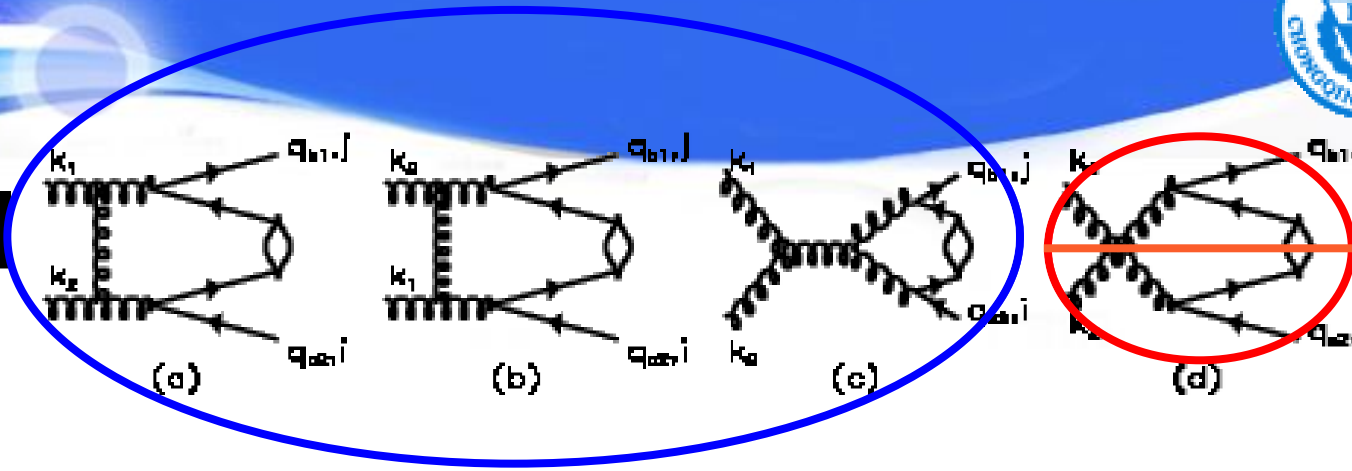

Key：QCD to QED diagrams

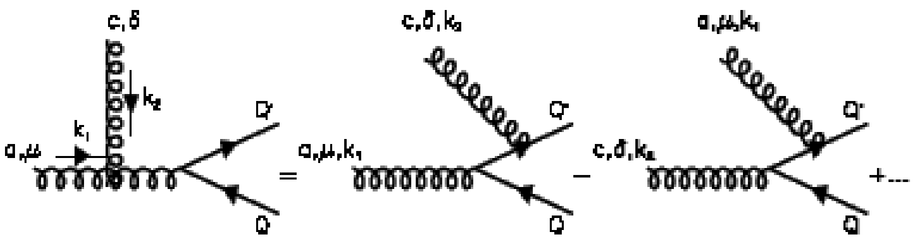

FIG. 6: The three-gluon coupling vertex is decomposed as in Eq.(16): the first two terms are the 'basic QED-like' terms and the 'remaining' terms are expressed by several extra basic functions.

A concrete example for decomposing Feynman diagrams

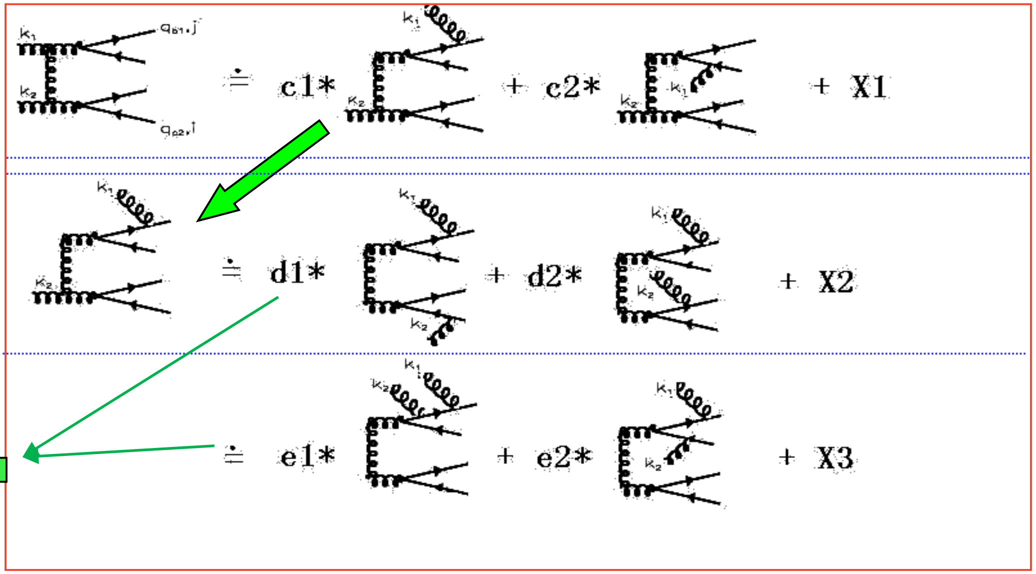

first step

second step

Equivalence of two ways get a relation among QED diagrams

Ten basic quark-lines

$$f_0(q_1,q_2,\lambda_1,\lambda_2) = \langle q_{0\lambda_1}|(\not{q}_1+m)\gamma_8(\not{q}_2-m)|q_{0\lambda_2}\rangle,$$

$$f_1(q_1,q_2,k,\lambda_1,\lambda_2,\lambda_3) = \langle q_{0\lambda_1}|(\not{q}_1+m)\gamma_8(\not{k}-\not{q}_2+m)\not{\epsilon}^{\lambda_3}(k,q_0)(\not{q}_2-m)|q_{0\lambda_2}\rangle,$$

$$f_2(q_1,q_2,k,\lambda_1,\lambda_2,\lambda_3) = \langle q_{0\lambda_1}|(\not{q}_1+m)\not{\epsilon}^{\lambda_3}(k,q_0)(\not{q}_1-\not{k}+m)\gamma_8(\not{q}_2-m)|q_{0\lambda_2}\rangle,$$

$$f_3(q_1,q_2,k,\lambda_1,\lambda_2,\lambda_3) = \langle q_{0\lambda_1}|(\not{q}_1+m)\not{\epsilon}^{\lambda_3}(k,q_0)(\not{q}_2-m)|q_{0\lambda_2}\rangle,$$

$$f_4(q_1,q_2,k_1,k_2,\lambda_1,\lambda_2,\lambda_3,\lambda_4) = \langle q_{0\lambda_1}|(\not{q}_1+m)\gamma_8(\not{k}_1+\not{k}_2-\not{q}_2+m)\not{\epsilon}^{\lambda_3}(k_1,q_0) \times (\not{k}_2-\not{q}_2+m)\not{\epsilon}^{\lambda_4}(k_2,q_0)(\not{q}_2-m)|q_{0\lambda_2}\rangle,$$

$$f_5(q_1,q_2,k_1,k_2,\lambda_1,\lambda_2,\lambda_3,\lambda_4) = \langle q_{0\lambda_1}|(\not{q}_1+m)\not{\epsilon}^{\lambda_3}(k_1,q_0)(\not{q}_1-\not{k}_1+m)\gamma_8 \times (\not{k}_2-\not{q}_2+m)\not{\epsilon}^{\lambda_4}(k_2,q_0)(\not{q}_2-m)|q_{0\lambda_2}\rangle,$$

$$f_6(q_1,q_2,k_1,k_2,\lambda_1,\lambda_2,\lambda_3,\lambda_4) = \langle q_{0\lambda_1}|(\not{q}_1+m)\not{\epsilon}^{\lambda_3}(k_1,q_0)(\not{q}_1-\not{k}_1+m) \times \not{\epsilon}^{\lambda_4}(k_2,q_0)(\not{q}_1-\not{k}_1-\not{k}_2+m)\gamma_8(\not{q}_2-m)|q_{0\lambda_2}\rangle,$$

$$f_7(q_1,q_2,k_1,k_2,\lambda_1,\lambda_2,\lambda_3,\lambda_4) = \langle q_{0\lambda_1}|(\not{q}_1+m)\gamma_8\not{\epsilon}^{\lambda_3}(k_1,q_0)\not{\epsilon}^{\lambda_4}(k_2,q_0)(\not{q}_2-m)|q_{0\lambda_2}\rangle,$$

$$f_8(q_1,q_2,k_1,k_2,\lambda_1,\lambda_2,\lambda_3,\lambda_4) = \langle q_{0\lambda_1}|(\not{q}_1+m)\not{\epsilon}^{\lambda_3}(k_1,q_0)\not{\epsilon}^{\lambda_4}(k_2,q_0)\gamma_8(\not{q}_2-m)|q_{0\lambda_2}\rangle,$$

$$f_9(q_1,q_2,k_1,k_2,\lambda_1,\lambda_2,\lambda_3,\lambda_4) = \langle q_{0\lambda_1}|(\not{q}_1+m)\not{\epsilon}^{\lambda_3}(k_1,q_0)\gamma_8\not{\epsilon}^{\lambda_4}(k_2,q_0)(\not{q}_2-m)|q_{0\lambda_2}\rangle.$$

Nine basic QED diagrams

$$E_{1,1,k} = f_1(q_{c1},q_{c2},k_1,\lambda_3,\lambda_4,\lambda_5)\cdot f_2(q_{b1},q_{b2},k_2,\lambda_1,\lambda_2,\lambda_6),$$

$$E_{2,1,k} = f_2(q_{c1},q_{c2},k_1,\lambda_3,\lambda_4,\lambda_5)\cdot f_2(q_{b1},q_{b2},k_2,\lambda_1,\lambda_2,\lambda_6),$$

$$E_{3,1,k} = f_1(q_{c1},q_{c2},k_1,\lambda_3,\lambda_4,\lambda_5)\cdot f_1(q_{b1},q_{b2},k_2,\lambda_1,\lambda_2,\lambda_6),$$

$$E_{4,1,k} = f_2(q_{c1},q_{c2},k_1,\lambda_3,\lambda_4,\lambda_5)\cdot f_1(q_{b1},q_{b2},k_2,\lambda_1,\lambda_2,\lambda_6),$$

$E_{5,1,k} =$ [illegible]

$E_{6,1,k} =$ [illegible]

$$E_{7,1,k} = f_0(q_{b1},q_{b2},\lambda_1,\lambda_2)\cdot f_5(q_{c1},q_{c2},k_1,k_2,\lambda_3,\lambda_4,\lambda_5,\lambda_6),$$

$$E_{8,1,k} = f_0(q_{b1},q_{b2},\lambda_1,\lambda_2)\cdot f_6(q_{c1},q_{c2},k_1,k_2,\lambda_3,\lambda_4,\lambda_5,\lambda_6),$$

$$E_{9,1,k} = f_0(q_{b1},q_{b2},\lambda_1,\lambda_2)\cdot f_7(q_{c1},q_{c2},k_1,k_2,\lambda_3,\lambda_4,\lambda_5,\lambda_6).$$

Seven are independent

$$E_{6,1,k} = E_{7,1,k} + 2q_{c2}\cdot k_2 E_{9,1,k} - E_{3,2,k} + E_{1,2,k},$$

$$E_{6,2,k} = E_{7,2,k} + 2q_{c2}\cdot k_1 E_{9,2,k} - E_{3,1,k} + E_{1,1,k},$$

$E_{6,3,k} = E_{7,3,k} + 2q_{b2}\cdot k_2 E_{9,3,k} - E_3$ [illegible]

$E_{6,4,k} = E_{7,4,k} + 2q_{c2}\cdot k_1 E_{9,4,k} - E_3$ [illegible]

and $E_{7,j,k}$ may be replaced as

$$E_{7,1,k} = -E_{4,1,k} + E_{2,1,k} + E_{8,1,k} - 2q_{c1}\cdot k_1(2E_{5,1,k} - 2E_{5,2,k} + E_{9,1,k}),$$

$$E_{7,2,k} = -E_{4,2,k} + E_{2,2,k} + E_{8,2,k} - 2q_{c1}\cdot k_2(2E_{5,2,k} - 2E_{5,1,k} + E_{9,2,k}),$$

$$E_{7,3,k} = -E_{4,3,k} + E_{2,3,k} + E_{8,3,k} - 2q_{b1}\cdot k_1(2E_{5,3,k} - 2E_{5,4,k} + E_{9,3,k}),$$

$$E_{7,4,k} = -E_{4,4,k} + E_{2,4,k} + E_{8,4,k} - 2q_{b1}\cdot k_2(2E_{5,4,k} - 2E_{5,3,k} + E_{9,4,k}).$$

The whole flowchart

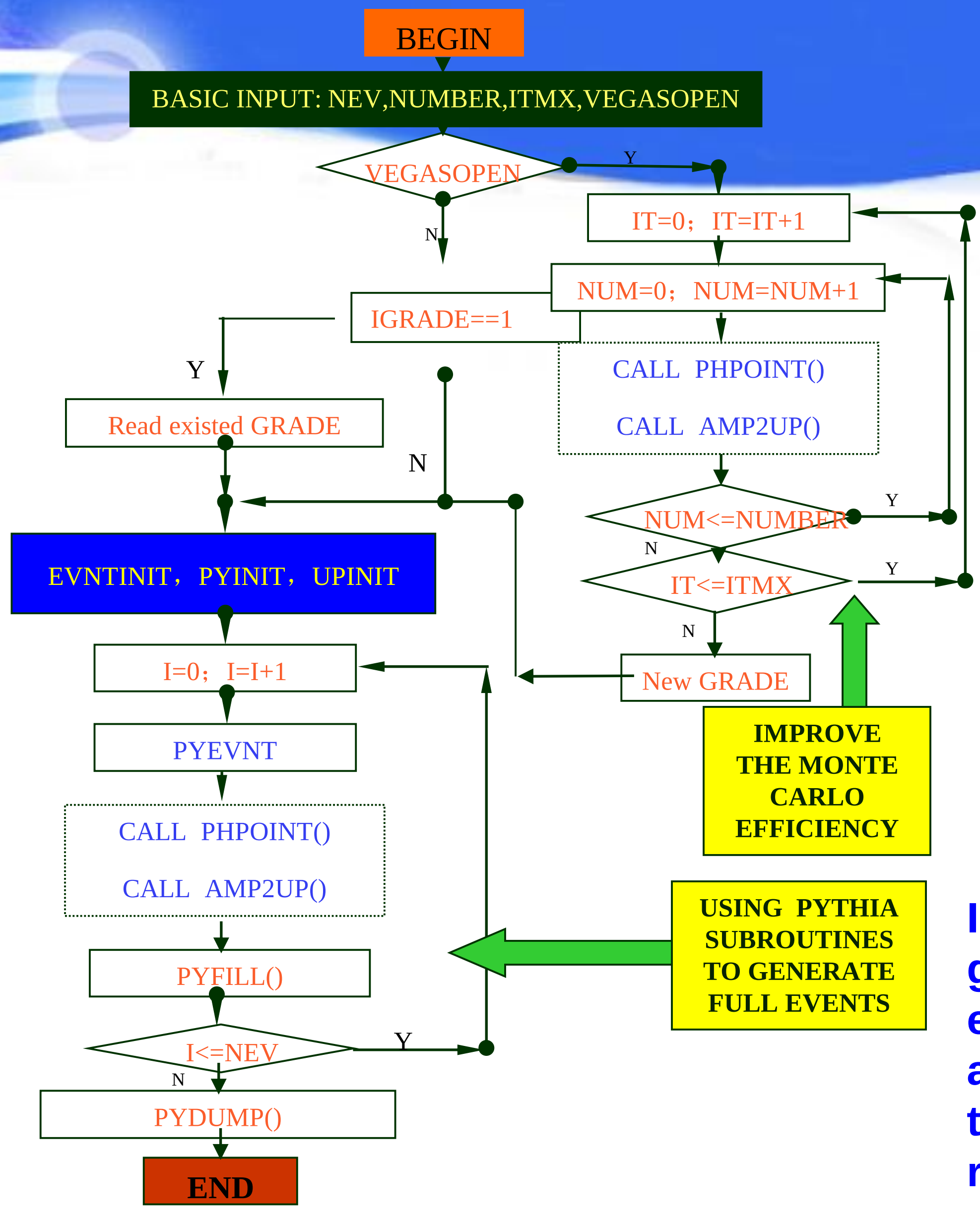

RABOS

VEGAS

Improve efficiency for generating unweighted events; The hit-and-miss approach for PYTHIA is time-consuming and is replaced by an alteration of MINT package.

As a summary

Because of

getting numerical results at the amplitude level

and

throughly applying all kind of symmetries

and

throughly maximizing the same type terms

and

properly using of ways to improve the sampling efficiency

GENXICC together with BCVEGPY
are high efficiency generators

3. Properties of hadroproduction of Xicc/Xibc

Numerical results under various input parameters could be conveniently obtained by using GENXICC

A cross-check of GENXICC at the subprocess level

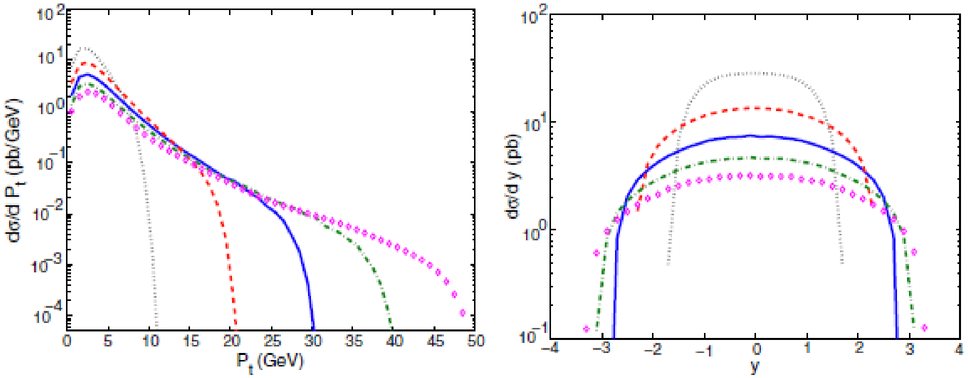

$E_{cm} = 20$ GeV, 40 GeV, 60 GeV, 80 GeV and 100 GeV,

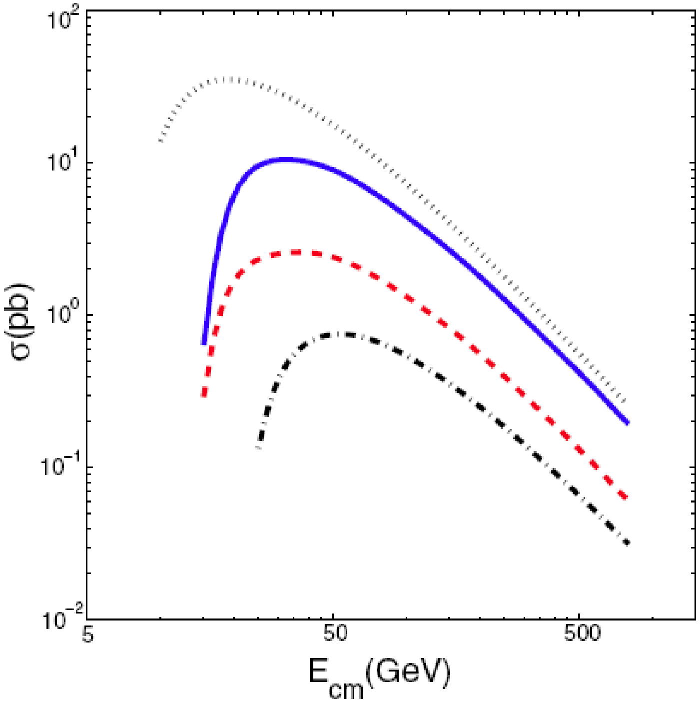

FIG. 5 (color online). The energy dependence of the integrated partonic cross-section for the production of the baryons via the heavy diquarks in terms of the gluon-gluon fusion mechanism. The dotted line, solid line, dashed line and dash-dot line stand for those via the diquarks $(cc)_{\bar{3}}[^3S_1]$, $(bc)_{\bar{3}}[^3S_1]$, $(bc)_{\bar{3}}[^1S_0]$ and $(bb)_{\bar{3}}[^3S_1]$ respectively. The curves for Ξ_{cc} and Ξ_{bb} both are divided by 2.

TABLE II. Cross sections (σ) for the hadronic production of Ξ_{cc} at colliders TEVATRON and LHC, where the (cc)-diquark is in $(cc)_{\bar{3}}[^3S_1]$ or $(cc)_6[^1S_0]$, and the symbol $g+c$ means $g+c \to \Xi_{cc}+\bar{c}$ and etc. In the calculations, cuts $p_t \geq 4$ GeV and $|y| \leq 1.5$ are taken at LHC, while at TEVATRON cuts $p_t \geq 4$ GeV, $|y| \leq 0.6$ instead.

–	TEVATRON ($\sqrt{S}=1.96$ TeV)		LHC ($\sqrt{S}=14.0$ TeV)	
–	$(cc)_{\bar{3}}[^3S_1]$	$(cc)_6[^1S_0]$	$(cc)_{\bar{3}}[^3S_1]$	$(cc)_6[^1S_0]$
$\sigma_{g+g}(nb)$	1.61	0.392	22.3	5.44
$\sigma_{c+g}(nb)$	2.29	0.360	22.1	3.42
$\sigma_{c+c}(nb)$	0.751	0.0431	8.74	0.475

Production at hadronic colliders

$$\text{diquark}: \sigma_{3S1}:\sigma_{1S0} \approx 4:1$$

c – quark contribution is sizable

Here *c*-quark is the extrinsic charm

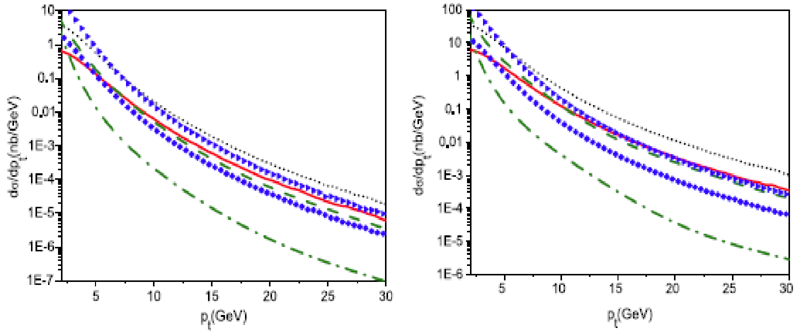

FIG. 9 (color online). The p_t-distribution for the hadroproduction of Ξ_{cc} at TEVATRON (left) and at LHC (right), where $|y| \leq 1.5$ at LHC and $|y| \leq 0.6$ at TEVATRON are adopted. The dotted line and the solid line are for gluon-gluon fusion mechanism, the triangle line and the diamond line are for $g+c \to \Xi_{cc}+\bar{c}$, the dashed line and the dash-dot line are for $c+c \to \Xi_{cc}+$ 'g', where the upper lines of each mechanism are for $(cc)_{\bar{3}}[^3S_1]$ and the lower lines are for $(cc)_6[^1S_0]$, respectively.

One subtle point: to avoid double counting

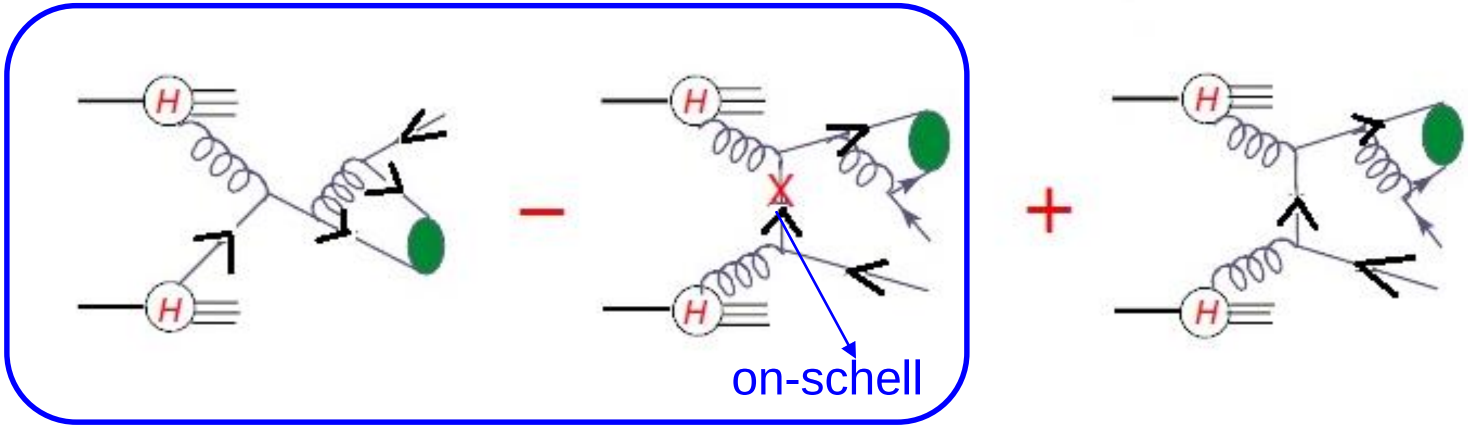

$$\sigma = F^{g}_{H_1}(x_1,\mu,m_c)F^{g}_{H_2}(x_2,\mu,m_c)\bigotimes\hat{\sigma}_{gg\to\Xi_{cc\{\bar{c}\bar{c}\}}}(x_1,x_2,\mu,m_c)+\Big\{\sum_{i,j=1,2;i\neq j}F^{g}_{H_i}(x_1,\mu,m_c)[F^{c}_{H_j}(x_2,\mu,m_c)$$

$$-F^{c}_{H_j}(x_2,\mu,m_c)_{\rm SUB}]\bigotimes\hat{\sigma}_{gc\to\Xi_{cc\{\bar{c}\}}}(x_1,x_2,\mu,m_c)\Big\}+\Big\{\sum_{i,j=1,2;i\neq j}[(F^{c}_{H_i}(x_1,\mu,m_c)-F^{c}_{H_i}(x_1,\mu,m_c)_{\rm SUB})$$

$$\cdot(F^{c}_{H_j}(x_2,\mu,m_c)-F^{c}_{H_j}(x_2,\mu,m_c)_{\rm SUB})]\bigotimes\hat{\sigma}_{cc\to\Xi_{cc\{g\}}}(x_1,x_2,\mu,m_c)\Big\}+\cdots,$$

$$F^{c}_{H}(x,\mu,m_c)_{\rm SUB}\equiv F^{g}_{H}(x,\mu,m_c)\bigotimes F^{c}_{g}(x,\mu,m_c)$$

$$=\int_x^1\frac{dy}{y}F^{c}_{g}(y,\mu,m_c)F^{g}_{H}\left(\frac{x}{y},\mu,m_c\right).$$

$$F^{c}_{g}(x,\mu,m_c)=\frac{\alpha_s(\mu)}{2\pi}\ln\frac{\mu^2}{m_c^2}P_{g\to c}(x)$$

$$P_{g\to c}(x)=\frac{1}{2}(1-2x+2x^2)$$

Production at SELEX

uses 600 GeV charged hyperon beam to produce charm particles in a set of thin foil targets of Cu or diamond—CME=33.58GeV

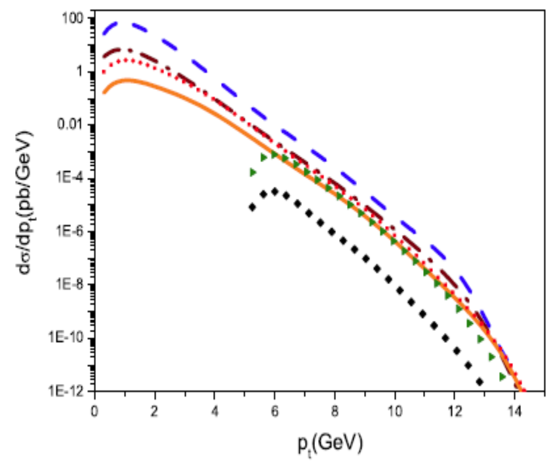

FIG. 10 (color online). The p_t-distributions for the hadroproduction of Ξ_{cc} at SELEX. The dotted line and the solid line are for gluon-gluon fusion mechanism, the dashed line and the dash-dot line are for $g + c \to \Xi_{cc} + \bar{c}$, the triangle line and the diamond line are for $c + c \to \Xi_{cc} + `g'$, where the upper lines of each mechanism are for $(cc)_{\bar{3}}[^3S_1]$ and the lower lines are for $(cc)_6[^1S_0]$, respectively.

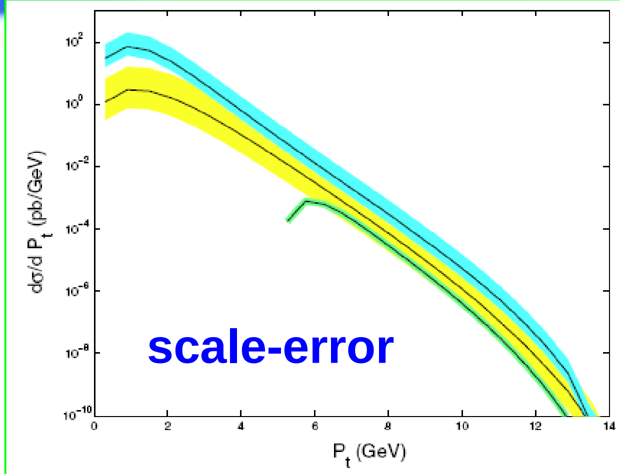

FIG. 11 (color online). The energy scale dependence of the p_t-distributions for each mechanism at SELEX, where the contributions from $(cc)_{\bar{3}}[^3S_1]$ and $(cc)_6[^1S_0]$ are summed up. The upper band is for the mechanism $g + c \to \Xi_{cc}$, the middle band is for gluon-gluon fusion mechanism and the lower band is for $c + c \to \Xi_{cc}$ mechanism, where the solid line in each band corresponds to $\mu = M_t$, the upper edge of the band is for $\mu = M_t/2$ and the lower edge is for $\mu = 2M_t$, respectively.

Extrinsic charm gives dominant contributions especially in low pT region

$$R = \frac{\sigma_{\rm total}}{\sigma_{gg\to\Xi_{cc}((cc)_{\bar{3}}[^3S_1])}},$$

TABLE IV. R values, which is defined in Eq. (10), for the hadronic production of Ξ_{cc}.

	SELEX	TEVATRON	LHC
-	$p_t > 0.2$ GeV	$p_t \geq 4$ GeV, $\|y\| \leq 0.6$	$p_t \geq 4$ GeV, $\|y\| \leq 1.5$
R	29	3.4	2.8

How about intrinsic charm ?

1980:BHPS-model

$$f_H^c(x,\mu) = f_H^{c,\mathrm{ex}}(x,\mu) + f_H^{c,\mathrm{in}}(x,\mu),$$
$$f_H^g(x,\mu) = f_H^{g,\mathrm{ex}}(x,\mu) + f_H^{g,\mathrm{in}}(x,\mu).$$

$$f_P^{c,\mathrm{in}}(x,2m_c) = f_P^{\bar{c},\mathrm{in}}(x,2m_c) = 6\xi[6x(1+x)\ln x + (1-x)(1+10x+x^2)]x^2, \quad (7)$$

where P stands for the proton, the parameter ξ is determined by the first momentum of the distribution, i.e., the probability to find a charm quark in total:

$$A_{\mathrm{in}} \equiv \int_0^1 f_P^{c,\mathrm{in}}(x,2m_c)\,\mathrm{d}x = \xi \times 1\%.$$

using DGLAP
get PDF at any scales

When $\xi = 1$, it means that the probability for finding $c/\bar{c}$ component in proton at the fixed low-energy scale $2m_c$ is 1% as suggested in [12, 13]. In the following, we will take a broader range $\xi \in [0.1, 1]$ to do our discussions[6]. The charm content in an anti-proton is the same as

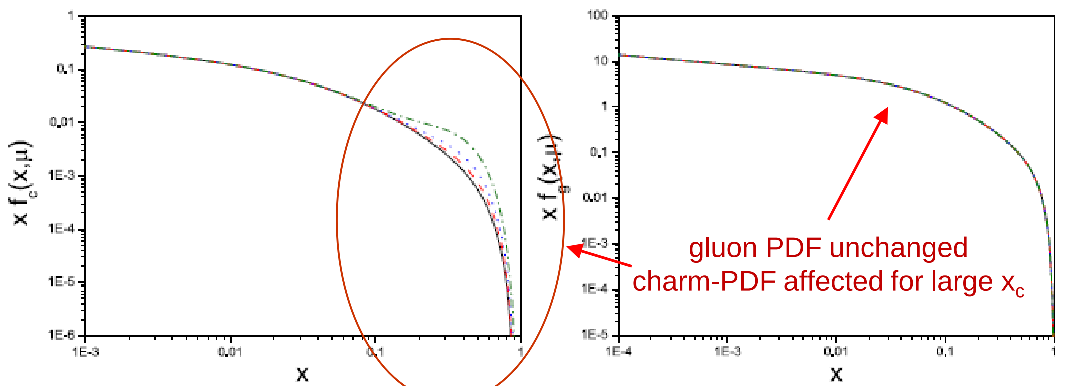

Figure 2. The charm PDF (left) and gluon PDF (right) at $\mu^2 = 10\ \mathrm{GeV}^2$. The solid line is for $xf_c^0(x,\mu)$ or $xf_g^0(x,\mu)$. The dashed line, the dotted line and the dash-dotted line are for $xf_c(x,\mu)$ or $xf_g(x,\mu)$ with $A_{\mathrm{in}} = 0.1\%, 0.3\%$ and 1%, respectively.

J.Pumplin, CTEQ, PRD73,114015(2006)

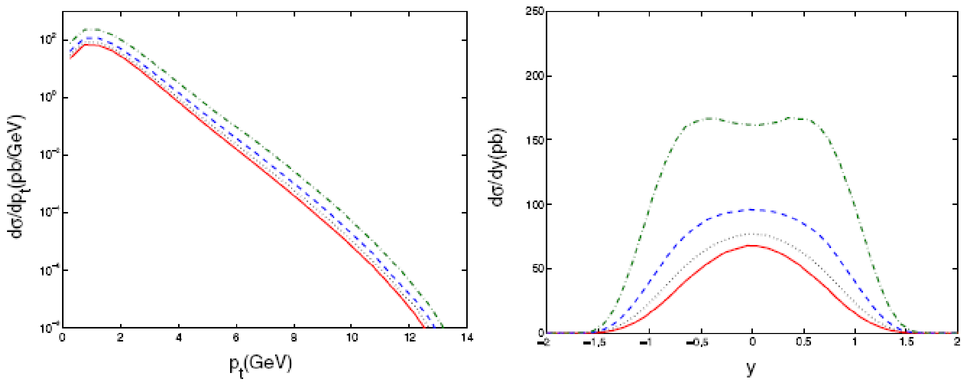

Figure 3. The p_t-distributions (left) and y-distributions (right) for the hadroproduction of Ξ_{cc} at SELEX with different values of $A_{\rm in}$. The dotted, the dashed and the dash-dotted lines are for $A_{\rm in} = 0.1\%, 0.3\%$ and 1%, respectively. The result with CTEQ6HQ, i.e., $A_{\rm in} = 0$ is shown by a solid line (the lowest one).

If there is intrinsic charm, the effect could be sizable for SELEX

Table 1. The contribution of σ_{ab} from different sub-processes initialized by the partons ab to the total cross section (in pb) for the Ξ_{cc} hadronic production at SELEX with the cut $p_t > 0.2$ GeV.

	CTEQ6HQ($A_{\rm in}=0$)			$A_{\rm in}=1\%$		
	σ_{gg}	σ_{cc}	σ_{gc}	σ_{gg}	σ_{cc}	σ_{gc}
$(cc)_{\bar{3}}[^3S_1]$	4.03	1.02×10^{-3}	102.	4.06	1.25×10^{-2}	372
$(cc)_6[^1S_0]$	0.754	4.15×10^{-5}	11.3	0.758	5.01×10^{-4}	40.9

Table 2. The contribution rates of the sub-process $gc\to\Xi_{cc}$ in the different x region in the charm quark PDFs with $A_{\rm in} = 1\%$ and $p_t > 0.2$ GeV.

$0.0\leqslant x_c\leqslant0.2$	$0.2\leqslant x_c\leqslant0.4$	$0.4\leqslant x_c\leqslant0.6$	$0.6\leqslant x_c\leqslant0.8$	$0.8\leqslant x_c\leqslant1.0$
25%	50%	22%	3%	~0

Table 3. The R values for SELEX with the cut $p_t > 0.2$ GeV.

	CTEQ6HQ ($A_{\rm in}=0$)	$A_{\rm in}=0.1\%$	$A_{\rm in}=0.3\%$	$A_{\rm in}=1\%$
R	29.3	36.6	51.3	103.

$$R = \frac{\sigma_{\rm total}}{\sigma_{gg\to\Xi_{cc}((cc)_{\bar{3}}[^3S_1])}},$$

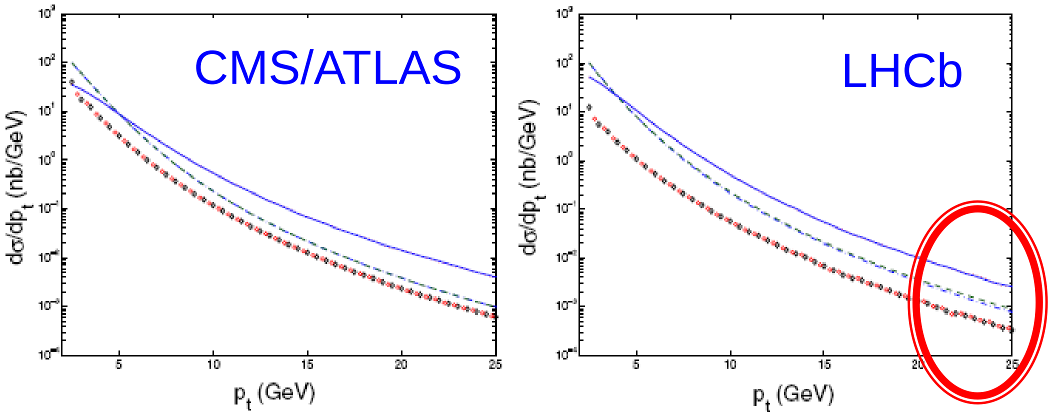

Figure 5. The p_t-distributions for the hadroproduction of Ξ_{cc} at LHC. The left figure is for CMS or ATLAS with the rapidity cut $|y| \leqslant 1.5$ being adopted and the right one is for LHCb with the pseudo-rapidity cut $1.8 \leqslant |\eta| \leqslant 5.0$ being adopted. The solid line, the dash-dotted line and the circle line correspond to that of the $g+g$, $g+c$ and $c+c$ mechanisms without the intrinsic charm being considered (the PDFs in CTEQ6HQ [8] are used), respectively. The dotted line, the dashed line and the diamond line correspond to that of the $g+g$, $g+c$ and $c+c$ mechanisms with the intrinsic charm being considered (the PDFs of equation (6) with $A_{\rm in} = 1\%$ are used), respectively. The differences with and without intrinsic charm are so small that, of them, only at LHCb for the $g+c$ mechanism the difference can be seen from the right figure.

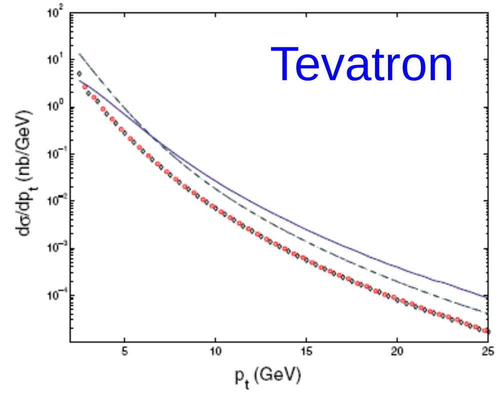

Figure 6. The p_t-distributions for the hadroproduction of Ξ_{cc} at TEVATRON with the rapidity cut $|y| \leqslant 0.6$ being adopted. The meaning for the lines in the figure is the same as figure 5. The differences between the two cases with and without intrinsic charm are too small to be seen.

LHC and TEVATRON are hard
to measure the difference
with or without intrinsic charm

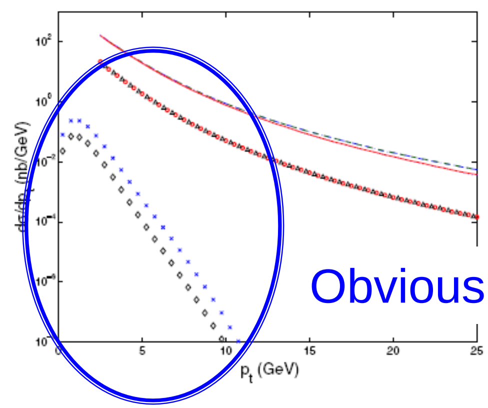

Figure 8. The p_t-distributions for the hadroproduction of Ξ_{cc}. The dotted line, the dash-dotted line, the circle line and the diamond line are those corresponding to LHCb, LHC, Tevatron and SELEX with $A_{\rm in} = 0$, respectively. The solid, the dashed line, the triangle line and the cross line are those corresponding to LHCb, LHC, Tevatron and SELEX with $A_{\rm in} = 1\%$, respectively. Only at SELEX, the difference between the cases with and without intrinsic charm can be seen.

The results at Aftre@LHC may clarify the puzzle of SELEX

Production of Xicc at the After@LHC

May test intrinsic charm mechanism

TABLE I. Total cross sections for the Ξ_{cc} production at the After@LHC with $\sqrt{S} \simeq 115$ GeV, where the intermediate (cc) diquark is in $[^3S_1]_{\bar{3}}$ or $[^1S_0]_{6}$, respectively. $m_c = 1.75$ GeV and $p_t > 0.2$ GeV.

	σ_{g+g} (pb)	σ_{g+c} (pb)	σ_{c+c} (pb)
$(cc)_{\bar{3}}[^3S_1]$	530	3.19×10^3	0.999
$(cc)_{6}[^1S_0]$	99.7	348	0.040

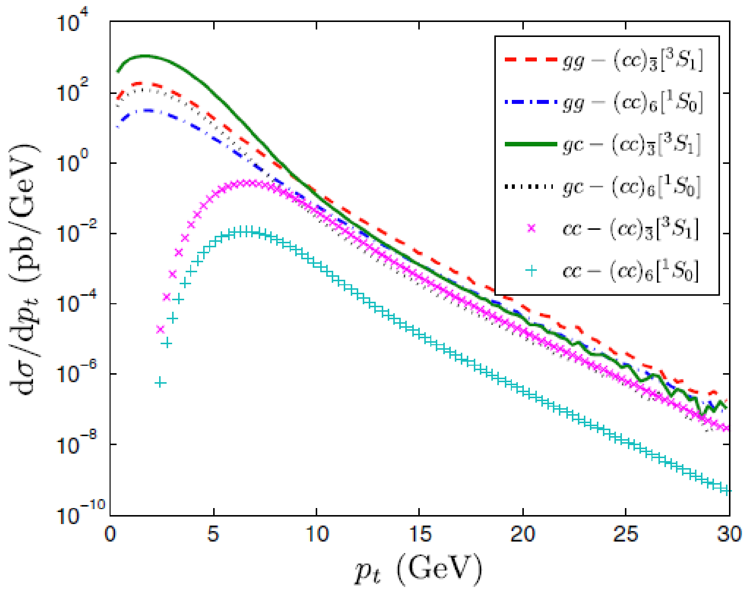

$$\sigma_{g+g} : \sigma_{g+c} : \sigma_{c+c} \simeq 6.1 \times 10^2 : 3.4 \times 10^3 : 1.$$

$$R = \frac{\sigma_{\rm total}}{\sigma_{gg \to \Xi_{cc}((cc)_{\bar{3}}[^3S_1])}},$$

A comparison of Xicc, Xibc, Xibb at the LHC (14TeV)
(similar for 7TeV, 8TeV)

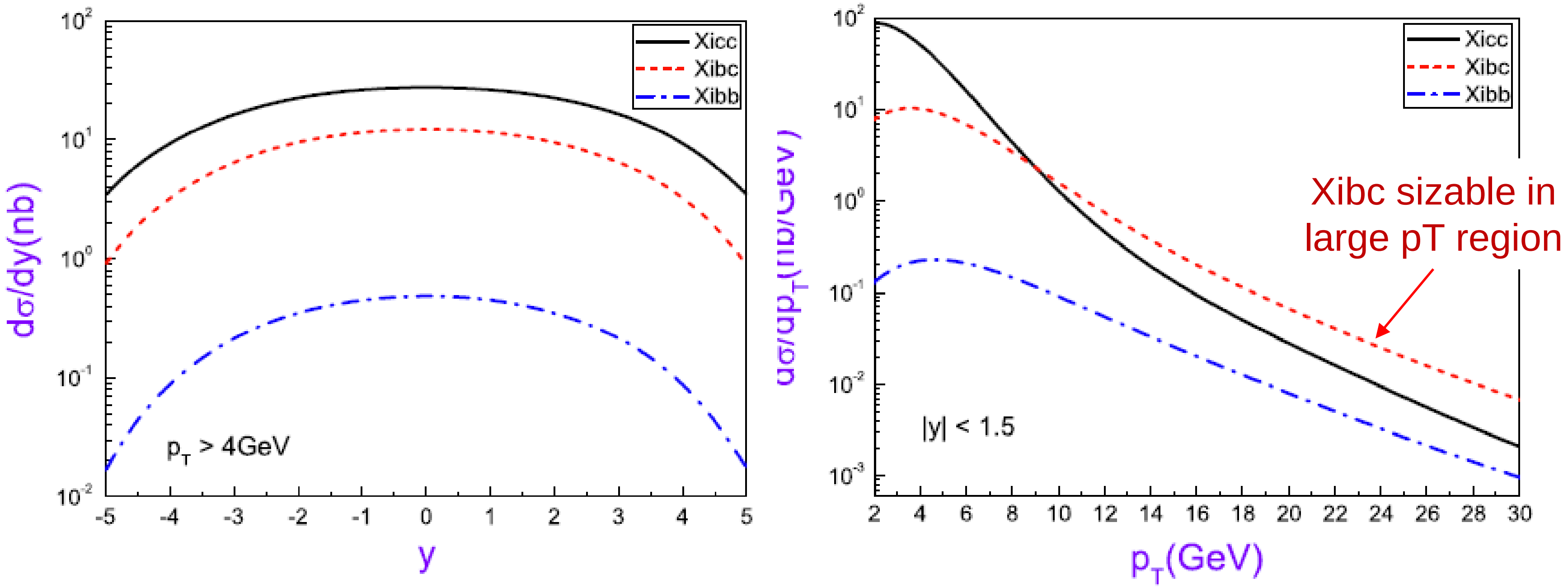

4. Summary and Prospects

- Due to its high efficiency, **GENXICC**, shall be very useful for MC simulation. **One can conveniently obtain results under various input parameters.**

- The coming more accurate LHC data shall provide a better platform to check all theoretical predications and to learn the Xicc properties in more detail.

- Together with its decay properties, we can obtain a full estimation of Xicc, and hence have a better comparison with SELEX experiment.

small pT

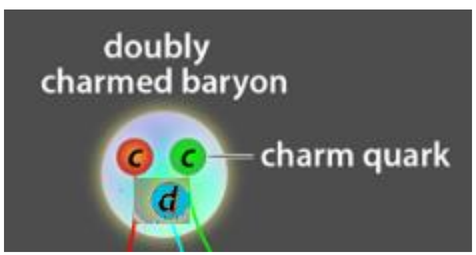

LHCb

$\Xi_{cc}^{++} = ccu$ →

← $\Xi_{cc}^{+} = ccd$

SELEX

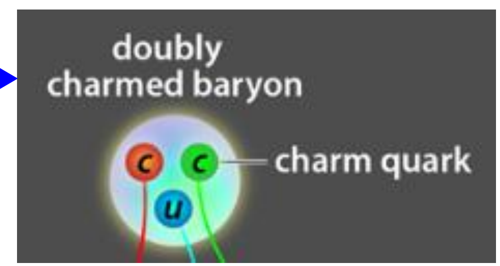

large pT

How to explain the puzzles between SELEX and LHCb ?
How to explain the ~100MeV mass difference between those two baryons ? Theoretically, it is several MeV
Why different availability at different platforms, since their production rate are theoretically the same?

Within LF-QCD, taking into intrinsic charm, may solve the spectrum problem/1709.09903

How to improve the precision of pQCD calculations

Principal of Maximum Conformality（PMC）
(Collaborators: Stanley J. Brodsky, Matin Mojaza, …)

Why insistent on using the guessed renormalization scale ? !
Can we achieve scheme-and-scale independent prediction at any fixed order ? !

Fixed-order prediction at the hadronic colliders

General factorization picture

$$d\sigma = f_a f_b \otimes \hat{\sigma} \otimes F$$

parton distribution functions

Perturbative partonic cross section (virtual & real radiation)

Fragmentation models

$$\hat{\sigma} = \sigma_0[1 + \alpha_s + \alpha_s^2 + \cdots]$$

How to set the renormalization scale ?

Contains α_s^n of tree level process

NLO

NNLO current frontier

Before and after applying the PMC, the issues are always like this

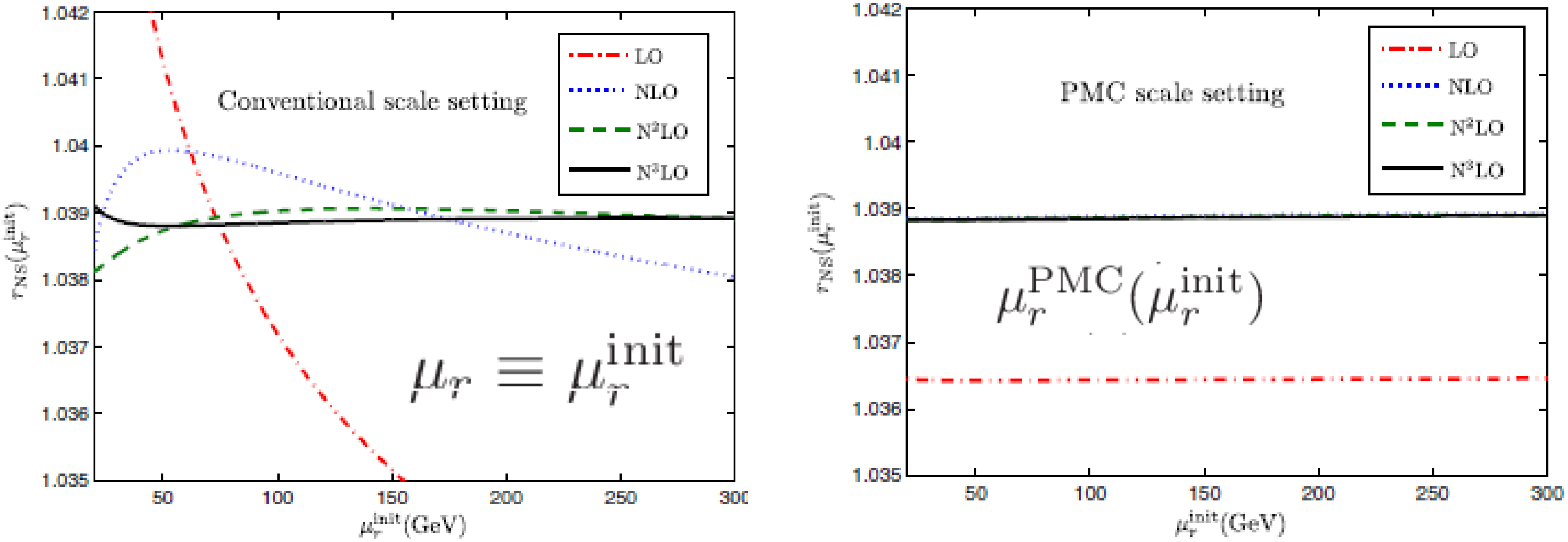

PMC predictions:
Quickly approaches its "true" value; also scheme-independent
More accurate predictions for low orders without initial scale dependence
Residual scale uncertainty is negligible

Hopefully, we may find time to discuss this topic

Thanks for your attention !

Works related

== GENXICC – A generator for hadronic production of Xicc, Xibc, Xibb bayons ==

1) << GENXICC1.0 …>> Comput.Phys.Commun.177, 467- 478 (2007)

2) << GENXICC2.0 …>> Comput.Phys.Commun.181, 1144-1149 (2010)

3) << GENXICC2.1 …>> Comput.Phys.Commun.184, 1070-1074 (2013)

======= Theoretical Predictions for SELEX, LHC and After@LHC =======

1) <<Estimate of the hadronic production of the doubly charmed baryon Xicc under GM-VFN scheme >> Phys.Rev.D73, 094022 (2006)

2) <<Hadronic production of the doubly charmed baryon Xicc with intrinsic charm >> J.Phys.G34, 845 (2007)

3) <<Hadronic Production of the Doubly Heavy Baryon Xibc at LHC>> Phys.Rev.D83, 034026 (2011)

4) <<Hadronic Production of Xicc at a Fixed-Target Experiment at the LHC >> Phys.Rev.D89, 074020 (2014)

=== Discussions their availability at the dfferent platforms ===

=== Super ZF, ILC and LHeC ===

1) <<Doubly Heavy Baryon Production at A High Luminosity e+e- Collider>>
   Phys.Rev.D73, 094022 (2012)

2) <<Further Study on the Doubly Heavy Baryon Production around the Z0 Peak at A High Luminosity e+e- Collider>>
   Phys.Rev.D87, 054027 (2013)

3) <<Photoproduction of Doubly Heavy Baryon at the ILC>>
   JHEP1412, 018(2014)

4) <<Photoproduction of Doubly Heavy Baryon at the LHeC >>
   Phys.Rev.D95, 074020(2017)